Analytical solution for an acoustic boundary layer around an oscillating rigid sphere

View Online　　　Export Citation　　　CrossMark

Evert Klaseboer,[1] 　 Qiang Sun (孙强),[2,a] 　 and Derek Y. C. Chan[3,4,b]

AFFILIATIONS

[1] Institute of High Performance Computing, 1 Fusionopolis Way, Singapore 138632, Singapore
[2] Australian Research Council Centre of Excellence for Nanoscale BioPhotonics, School of Science, RMIT University, Melbourne, VIC 3001, Australia
[3] School of Mathematics and Statistics, University of Melbourne, Parkville, VIC 3010, Australia
[4] Department of Mathematics, Swinburne University of Technology, Hawthorn, VIC 3121, Australia

[a] Author to whom correspondence should be addressed: qiang.sun@rmit.edu.au
[b] Electronic mail: D.Chan@unimelb.edu.au. URL: http://D.Chan.is

ABSTRACT

Analytical solutions in fluid dynamics can be used to elucidate the physics of complex flows and to serve as test cases for numerical models. In this work, we present the analytical solution for the acoustic boundary layer that develops around a rigid sphere executing small amplitude harmonic rectilinear motion in a compressible fluid. The mathematical framework that describes the primary flow is identical to that of wave propagation in linearly elastic solids, with the difference being the appearance of complex instead of real valued wave numbers. The solution reverts to the well-known classical solutions in special limits: the potential flow solution in the thin boundary layer limit, the oscillatory flat plate solution in the limit of large sphere radius, and the Stokes flow solutions in the incompressible limit of infinite sound speed. As a companion analytical result, the steady second order acoustic streaming flow is obtained. This streaming flow is driven by the Reynolds stress tensor that arises from the axisymmetric first order primary flow around such a rigid sphere. These results are obtained with a linearization of the non-linear Navier–Stokes equations valid for small amplitude oscillations of the sphere. The streaming flow obeys a time-averaged Stokes equation with a body force given by the Nyborg model in which the above-mentioned primary flow in a compressible Newtonian fluid is used to estimate the time-averaged body force. Numerical results are presented to explore different regimes of the complex transverse and longitudinal wave numbers that characterize the primary flow.

Published under license by AIP Publishing. https://doi.org/10.1063/5.0033933

I. INTRODUCTION

Acoustic streaming is the steady flow generated by periodic small amplitude Rayleigh acoustic fields in compressible Newtonian fluids. In certain flow regimes, the streaming patterns are observed as intricate steady vortices or circulatory patterns near solid boundaries. The creation of a steady streaming flow due to a periodic acoustic wave is inherently a non-linear effect that arises from the time-averaged velocity field governed by the time-dependent Navier–Stokes equations. The role of fluid viscosity and the generation of vorticity near solid boundaries are key to the streaming phenomenon so that the details of such flow depend on the geometry of the system and on the hydrodynamic boundary

conditions. Consequently, the flow characteristics will vary near solid or soft surfaces such as biological cell membranes, bubble surfaces, or fluid interfaces and as such can provide very different modes of steady fluid transport. Recent advances in microfluidics and ultrasonic technologies stimulated resurgent interest in these phenomena.[1–8]

From the point of view of analytical and numerical analyses, acoustic streaming has also attracted renewed interest recently, for example, around spheres, bubbles, and drops,[9,10] including thermal effects.[11,12] Previous studies of steady streaming around a stationary sphere considered an imposed external oscillatory flow field[13,14] or streaming around bubbles and drops.[15,16] The amplitude of the oscillations is also assumed to be small compared to the sphere radius. As

the fluid is generally taken to be incompressible, this is termed steady streaming rather than acoustic streaming.[17] Streaming around a stationary sphere in a compressible fluid has been considered by Lee and Wang.[18] However, they made a further assumption to only consider the flow outside the boundary layer to simplify the analysis.

To elucidate the physics of such complex flows, it is instructive to have available analytical solutions for special cases that can also serve as test cases for more complex numerical models. It turns out that the governing equations and boundary conditions for an oscillating rigid sphere in an infinite but otherwise quiescent compressible Newtonian fluid are very similar to those of a rigid sphere undergoing oscillatory motion in an infinite linear elastic material for which an analytical solution has recently been given by Klaseboer *et al.*[19]

This oscillatory motion of a sphere in a compressible Newtonian fluid generates both an acoustic field due to compressibility of the fluid and an acoustic boundary layer in the fluid near the sphere due to viscosity. Without further approximations, we can construct an analytic solution that accounts for the transition from viscous boundary layer dominated flow near interfaces to near potential flow far from boundaries. The known limits of negligible viscosity, negligible compressibility, or zero frequency can be recovered as special cases. In the geometric limit of a large sphere, results for both normal and tangential flows at a planar surface are obtained at different parts of the sphere. To the best knowledge of the authors, such a theoretical solution has not appeared in the literature before. Taking this analytical solution to be the primary solution, we then obtain an expression for the secondary flow or acoustic streaming that originates from small non-linear inertial effects.

At low amplitudes of oscillation,[20] the streaming flow can be obtained as a non-linear steady secondary correction to the linear time-dependent primary flow. In this paper, we present a general analytic solution of the model[21] for streaming flow in a compressible Newtonian fluid around a rigid sphere with a radius, a that is executing rectilinear oscillatory motion with an angular frequency $\omega \equiv 2\pi f$ and a velocity amplitude U_0. We focus on the Rayleigh[22] or acoustic limit in which the magnitude of the sphere displacement U_0/ω is small compared to the sphere radius a and also on the low Reynolds number regime where the non-linear inertial term in the Navier–Stokes equation is small.

In Sec. II, we recapitulate the Nyborg formulation for the steady acoustic streaming flow as a second order effect driven by a linear primary flow. In Sec. III, symmetry arguments pertaining to the periodic primary flow due to a rigid sphere executing rectilinear oscillations are used to construct the time-averaged Reynolds stress that results in a steady body force in a Stokes equation that governs the steady streaming velocity field. Possible acoustic waves inside the rigid sphere are not taken into account. An explicit analytic solution for periodic primary flow is given in Sec. III B. Corresponding general solutions for the steady acoustic streaming flow (using the theory of electrophoresis of a charged spherical colloidal particle[23,24]) are outlined in Sec. III D and are further worked out in the Appendix. The solutions for the streaming vorticity and velocity are expressed explicitly as integrals of the body force. Analytic and numerical results for the primary flow around a rigid sphere are given in Sec. IV. The reduction in this general solution to special cases and geometric limits together with numerical comparisons are detailed in Sec. V, and the concluding remarks are given in Sec. VI.

II. THE NYBORG FRAMEWORK

The Nyborg framework,[21] based on the earlier Eckart theory,[25] describes the transmission of an acoustic wave in a compressible Newtonian fluid with constant shear viscosity μ and bulk viscosity μ_B. The governing equations for the space and time-dependent density, $\bar{\rho}(\boldsymbol{x}, t)$, velocity field, $\bar{\boldsymbol{v}}(\boldsymbol{x}, t)$, and pressure, $\bar{p}(\boldsymbol{x}, t)$, are the continuity and momentum equations,

$$\frac{\partial \bar{\rho}}{\partial t} + \nabla \cdot (\bar{\rho}\, \bar{\boldsymbol{v}}) = 0, \tag{1a}$$

$$\frac{\partial (\bar{\rho}\, \bar{\boldsymbol{v}})}{\partial t} + \nabla \cdot (\bar{\rho}\, \bar{\boldsymbol{v}}\, \bar{\boldsymbol{v}}) = -\nabla \bar{p} + \mu \nabla^2 \bar{\boldsymbol{v}} + \left(\mu_B + \frac{1}{3}\mu\right)\nabla(\nabla \cdot \bar{\boldsymbol{v}}). \tag{1b}$$

At small vibrating amplitudes, for which all physical quantities can be linearized about their equilibrium values in terms of the small parameters: $\epsilon = |\nabla \cdot (\bar{\rho}\, \bar{\boldsymbol{v}}\, \bar{\boldsymbol{v}})|/|\partial(\bar{\rho}\, \bar{\boldsymbol{v}})/\partial t| \sim U_0/(a\omega) \ll 1$, and the Reynolds number, $Re = |\nabla \cdot (\bar{\rho}\, \bar{\boldsymbol{v}}\, \bar{\boldsymbol{v}})|/|\mu \nabla^2 \bar{\boldsymbol{v}}| \sim \rho_0 a U_0/\mu \ll 1$, all quantities in (1) are expanded in powers of ϵ about the constant reference density ρ_0 and pressure p_0, and noting that the reference velocity is zero,

$$\bar{\rho} = \rho_0 + \epsilon\, \bar{\rho}_1 + \epsilon^2\, \bar{\rho}_2 + \dots, \quad \bar{p} = p_0 + \epsilon\, \bar{p}_1 + \epsilon^2\, \bar{p}_2 + \cdots,$$
$$\bar{\boldsymbol{v}} = \epsilon\, \bar{\boldsymbol{v}}_1 + \epsilon^2\, \bar{\boldsymbol{v}}_2 + \dots. \tag{2}$$

To order ϵ, we have the equations that govern the primary flow,

$$\frac{\partial \bar{\rho}_1}{\partial t} + \rho_0 \nabla \cdot \bar{\boldsymbol{v}}_1 = 0, \tag{3a}$$

$$\rho_0 \frac{\partial \bar{\boldsymbol{v}}_1}{\partial t} = -\nabla \bar{p}_1 + \mu \nabla^2 \bar{\boldsymbol{v}}_1 + \left(\mu_B + \frac{1}{3}\mu\right)\nabla(\nabla \cdot \bar{\boldsymbol{v}}_1). \tag{3b}$$

For the case of the primary velocity field $\bar{\boldsymbol{v}}_1(\boldsymbol{x}, t)$ that is driven by a sphere of radius, a, executing rectilinear oscillatory motion with a center of mass velocity: $\boldsymbol{U}_0 e^{-i\omega t} = U_0 e^{-i\omega t}\boldsymbol{e}_z$, along the z direction in a compressible Newtonian fluid, we now show that this primary flow can be obtained analytically due to axial symmetry. We assume harmonic time dependence in all primary flow quantities: $\bar{\rho}_1(\boldsymbol{x}, t) \sim \rho(\boldsymbol{x})e^{-i\omega t}$, $\bar{p}_1(\boldsymbol{x}, t) \sim p(\boldsymbol{x})e^{-i\omega t}$, and $\bar{\boldsymbol{v}}_1(\boldsymbol{x}, t) \sim \boldsymbol{u}(\boldsymbol{x})e^{-i\omega t}$, so that the order ϵ [Eq. (3)] becomes

$$-i\omega\rho + \rho_0 \nabla \cdot \boldsymbol{u} = 0, \tag{4a}$$

$$-i\omega\rho_0 \boldsymbol{u} = -\nabla p + \mu \nabla^2 \boldsymbol{u} + \left(\mu_B + \frac{1}{3}\mu\right)\nabla(\nabla \cdot \boldsymbol{u}). \tag{4b}$$

For small amplitude acoustic waves, we can assume the equation of state: $\nabla p(\boldsymbol{x}) = c_0^2 \nabla \rho(\boldsymbol{x})$, where $c_0 > 0$ is the constant speed of sound in the fluid. This assumes that adiabatic conditions hold.[26] The pressure p can thus be eliminated from (4) to give[27]

$$[(k_T^2/k_L^2) - 1]\nabla(\nabla \cdot \boldsymbol{u}) + \nabla^2 \boldsymbol{u} + k_T^2 \boldsymbol{u} = \boldsymbol{0}, \tag{5}$$

with (complex) transverse k_T and longitudinal k_L wave numbers defined by

$$k_T^2 \equiv i\frac{\rho_0 \omega}{\mu} \quad \text{and} \quad k_L^2 \equiv \omega^2 \bigg/ \left[c_0^2 - \frac{i\omega}{\rho_0}\left(\mu_B + \frac{4}{3}\mu\right)\right]. \tag{6}$$

Note that $|k_L^2| \leq (3/4)|k_T^2|$ and that the viscous penetration depth defined as $\delta = \sqrt{2\mu/(\rho_0\omega)}$[28] is closely related to the Womersley number M[14,29] as $|M| = \sqrt{2}a/\delta = |k_T|a$. In Sec. III, Eq. (5) will be solved for a rigid sphere executing periodic rectilinear motion with no-slip fluid boundary conditions such that boundary layers are specifically taken into account.

III. FORMAL SOLUTION FOR AXISYMMETRIC FLOW

In this section, we exploit the axial symmetry condition of the primary flow driven by the rectilinear motion of a rigid sphere to construct a general formal solution of the problem. We draw on a previously obtained solution for a rigid sphere oscillating in an infinite linearly elastic (solid mechanics) domain.

A. Symmetry of the first order primary flow

The solution of the order ϵ [Eq. (5)] due to the oscillatory motion of a rigid sphere along the z direction with velocity amplitude U_0 can only depend on the vector U_0 and the position vector x with the origin at the center of the sphere. Symmetry consideration implies that the solution to (5) has the general form

$$u(x) = u_r(r)\cos\theta\, e_r + u_\theta(r)\sin\theta\, e_\theta$$

$$= \left\{ -\frac{2}{r}h(r) + \frac{\mathrm{d}\phi(r)}{\mathrm{d}r} \right\} U_0 \cos\theta\, e_r$$

$$+ \left\{ \frac{1}{r}\frac{\mathrm{d}}{\mathrm{d}r}[rh(r)] - \frac{\phi(r)}{r} \right\} U_0 \sin\theta\, e_\theta, \quad (7)$$

where $u_r(r)$ and $u_\theta(r)$ are only functions of the radial distance r from the center of the sphere and e_r and e_θ are unit vectors in the direction of increasing radial and polar coordinates relative to the z direction. In general, a vector field u can be expressed as the sum of a divergence-free component u_T with $\nabla \cdot u_T = 0$ and an irrotational component u_L with $\nabla \times u_L = 0$, as shown by Landau and Lifshitz[30] (pp. 101–106, Sec. 22). Since $u(x)$ is independent of the azimuthal angle φ and has no components in the e_φ direction, the irrotational longitudinal component of u can be represented as $u_L(x) = \nabla[\phi(r)\cos\theta]U_0$, where $\phi(r)$ satisfies $(\nabla^2 + k_L^2)[\phi(r)\cos\theta] = 0$. Similarly, the divergence-free transverse component of the velocity can be represented as $u_T(x) = -\nabla \times [h(r)\sin\theta\, e_\varphi]U_0$, with $(\nabla^2 + k_T^2)[h(r)\cos\theta] = 0$. Representation (7) then follows.

The introduction of $\phi(r)$ and $h(r)$ simplifies the expression for the pressure and the vorticity of the primary flow. From the continuity equation and the equation of state of the compressible fluid, the pressure is

$$p(x) = \frac{\rho_0 c_0^2}{i\omega}\nabla \cdot u(x) = \frac{\rho_0 c_0^2}{i\omega}\nabla^2[\phi(r)\cos\theta]\, U_0$$

$$= \frac{i\rho_0 c_0^2}{\omega}k_L^2\phi(r)\cos\theta\, U_0. \quad (8)$$

The pressure in the incompressible limit where $\nabla \cdot u \rightarrow 0$ and the speed of sound $c_0 \rightarrow \infty$ reduces to the familiar acoustic result: $p(x) = i\omega\rho_0\phi(r)\cos\theta U_0$. From (7), we find for the vorticity,

$$w(x) \equiv \nabla \times u(x) = -\frac{\mathrm{d}}{\mathrm{d}\theta}\left\{\nabla^2[h(r)\cos\theta]\right\}U_0\, e_\varphi$$

$$= -k_T^2 h(r)\sin\theta\, U_0\, e_\varphi. \quad (9)$$

The order ϵ [Eq. (5)] that governs the primary flow $u(x)$ has the same mathematical form as the equation for elastic waves in linear elasticity if the longitudinal and transverse velocities of the elastic waves are identified formally as $c_T^2 \equiv \omega^2/k_T^2$ and $c_L^2 \equiv \omega^2/k_L^2$, respectively. This analogy is explored further in Sec. III B.

B. The analogy with dynamic linear elasticity

In a linear dynamic elastic system, equilibrium of forces requires $\nabla \cdot \Sigma = \rho\partial^2 U/\partial t^2$, with Σ being the stress tensor, U being the displacement, ρ being the density, and t being the time. Assuming harmonic motion with angular frequency ω, one can write $\Sigma = \sigma e^{-i\omega t}$ and $U = u e^{-i\omega t}$, and then, (in the frequency domain) the equation of motion becomes $\nabla \cdot \sigma = -\rho\omega^2 u$. Linear isotropic homogeneous materials satisfy Hooke's law as follows:

$$\frac{\sigma}{\mu} = \left[\frac{k_T^2}{k_L^2} - 2\right](\nabla \cdot u)I + \nabla u + [\nabla u]^T, \quad (10)$$

with μ being the shear modulus, I being the identity matrix, and superscript "T" indicating the transpose. The longitudinal (k_L) and transverse (k_T) wave numbers in linear elasticity are defined as $k_L^2 = \omega^2\rho/(\lambda + 2\mu)$ and $k_T^2 = \omega^2\rho/\mu$ (λ is one of the Lamé constants) and are real valued quantities. When Hooke's law is substituted into the equation of motion, one gets

$$[(k_T^2/k_L^2) - 1]\nabla(\nabla \cdot u) + \nabla^2 u + k_T^2 u = 0. \quad (11)$$

This equation is identical to (5). Since the boundary conditions are also identical ($u = U_0$), these two systems should have identical mathematical solutions. In the work of Klaseboer et al.,[19] an analytical solution was given for the elastic waves emitted by a rigid sphere oscillating in an infinite elastic medium. The solution of the elastic wave problem can be represented as a combination of the Green's function and a dipole field, and explicit solutions for the velocity components were given by Klaseboer et al.[19] as

$$u = c_1 2\frac{a}{r}\left\{ e^{ik_T r}\left([1 + G(k_T r)]U_0 + F(k_T r)\frac{x \cdot U_0}{r^2}x\right)\right.$$

$$\left. - e^{ik_L r}\frac{k_L^2}{k_T^2}\left(G(k_L r)U_0 + F(k_L r)\frac{x \cdot U_0}{r^2}x\right)\right\}$$

$$- c_2\frac{a^3}{r^3}e^{ik_L r}\left\{(ik_L r - 1)U_0 + k_L^2 F(k_L r)(x \cdot U_0)x\right\}, \quad (12)$$

with the functions $F(y) \equiv -1 - 3i/y + 3/y^2$, $G(y) \equiv i/y - 1/y^2$, and x being the position vector with respect to the center of the sphere. This solution will also be valid in the acoustic boundary layer context. Note, however, that in linear elasticity, k_L and k_T are real parameters, while in the current case of acoustic streaming, they are complex parameters, as given in Eq. (6).

C. Solution for the primary flow

When an axial symmetric coordinate system is used, using $U_0 = U_0\cos\theta e_r - U_0\sin\theta e_\theta$, $x = re_r$, and $(x \cdot U_0) = rU_0\cos\theta$, Eq. (12)

becomes

$$\frac{u_\theta(r)}{U_0} = C_1 \frac{a}{r} \left[1 + G(k_T r) \right] e^{i k_T r} + C_2 \frac{a}{r} G(k_L r) e^{i k_L r}, \qquad (13a)$$

$$\frac{u_r(r)}{U_0} = 2 C_1 \frac{a}{r} G(k_T r) e^{i k_T r} + C_2 \frac{a}{r} \left[1 + 2G(k_L r) \right] e^{i k_L r}. \qquad (13b)$$

It is more convenient, instead of the constants c_1 and c_2 of Eq. (12), to introduce new constants $C_1 = -2c_1$ and $C_2 = k_L^2 a^2 \left[c_1 2/(k_T^2 a^2) + c_2 \right]$ in (13). The functions $h(r)$ and $\phi(r)$ defined in (7) can now be seen as

$$h(r) = -C_1 \, a \, G(k_T r) \, e^{i k_T r}, \qquad \phi(r) = -C_2 \, a \, G(k_L r) \, e^{i k_L r}. \qquad (14)$$

From the no-slip boundary conditions at the surface $r = a$: $u_r(a) = U_0$ and $u_\theta(a) = -U_0$, we find

$$C_1 = -\frac{\left[1 + 3G(k_L a) \right]}{\left[1 + G(k_T a) + 2G(k_L a) \right]} e^{-i k_T a},$$

$$C_2 = \frac{\left[1 + 3G(k_T a) \right]}{\left[1 + G(k_T a) + 2G(k_L a) \right]} e^{-i k_L a}. \qquad (15)$$

The complex valued k_T and k_L are taken to have positive imaginary parts to ensure a finite solution at infinity. We can now also identify terms in $\exp(i k_L r)$ and $\exp(i k_T r)$ to be the longitudinal, u_L, and transverse, u_T, components of u, respectively.

Solutions (13) and (14) reduce to potential flow solutions when $|k_T a| \gg 1$, as shown in Sec. V A. When the radius a is large, at $\theta = \pi/2$, the Stokes solution for an oscillating plate is recovered, and at $\theta = 0$, a plane sound wave is recovered, as illustrated in Sec. V B. In the incompressible limit, we recover the result given by Landau and Lifshitz[31] (p. 89, Sec. 24, Problem 5) and Stokes flow if the frequency ω tends to zero, as demonstrated in Sec. V C. The recovery of these classical solutions gives us further confidence that the constructed solution is indeed correct.

If the sphere has a zero tangential stress boundary condition, the vanishing of the tangential stress due to the primary flow will determine different constants C_1 and C_2.

D. Solution procedure for the secondary flow

The secondary "streaming" flow will now be obtained, assuming that the primary flow is as given in Sec. III C. The streaming velocity is determined by the order ϵ^2 terms of the momentum equation [Eq. (1b)],

$$\rho_0 \frac{\partial \overline{v}_2}{\partial t} + \frac{\partial (\overline{\rho}_1 \overline{v}_1)}{\partial t} + \rho_0 \, \nabla \cdot (\overline{v}_1 \, \overline{v}_1)$$

$$= -\nabla \overline{p}_2 + \mu \nabla^2 \overline{v}_2 + \left(\mu_B + \frac{1}{3} \mu \right) \nabla (\nabla \cdot \overline{v}_2). \qquad (16)$$

For harmonic time dependence of all quantities: $\overline{\phi}(x, t) \sim e^{-i \omega t}$, we define the corresponding steady, time-independent streaming quantities by taking the time average: $\phi(x) \equiv < \overline{\phi}(x, t) > = (1/T) \int_0^T \overline{\phi}(x, t) \, dt$, over one period of oscillation: $T = 1/f = 2\pi/\omega$.

By time averaging the order ϵ^2 momentum equation (16), we obtain the desired Stokes equation relating the time-averaged body force, $\mathcal{F}(x)$, to the time-average pressure, $P(x) \equiv < \overline{p}_2(x, t) >$, and the streaming velocity, $U(x) \equiv \langle \overline{v}_2(x, t) \rangle$,

$$\mathcal{F}(x) \equiv \rho_0 \, \nabla \cdot \langle \overline{v}_1 \, \overline{v}_1 \rangle = -\nabla P(x) + \mu \nabla^2 U(x). \qquad (17)$$

Since $\partial(\overline{\rho}_1 \, \overline{v}_1)/\partial t$ and $\partial(\overline{v}_2)/\partial t$ are periodic, their time average is zero. The time averaging also removes the periodic part of $(\overline{v}_1 \, \overline{v}_1)$, $\overline{p}_2(x, t)$ and $\overline{v}_2(x, t)$. Furthermore, the streaming velocity, $U(x)$ is divergence free, $\nabla \cdot U = 0$,[18,21] based on a physical argument that there are no steady sources or sinks. However, a formal proof of this result is not that straightforward. The secondary velocity satisfies $\nabla \cdot U(x) = -\nabla \cdot < \overline{v}_1 \overline{\rho}_1 > /\rho_0$. Thus it appears that both sides of this equation are of order ϵ^2. While Nyborg[21] assumed a solenoidal secondary flow from the onset, Lee and Wang[18] proved more rigorously that $\nabla \cdot U(x) = 0$ using a low viscosity argument.

Accepting that the streaming velocity U is divergence-free, its governing equation (17) is identical to a Stokes flow in the presence of a non-conservative body force $\mathcal{F}$ due to the time-averaged Reynolds stress tensor $\langle -\rho_0(\overline{v}_1 \, \overline{v}_1) \rangle$ that is given in terms of the first order velocity field $\overline{v}_1$.

This is the starting point for the general small amplitude theory of the streaming velocity by calculating $\mathcal{F}$ from the solution of the primary flow. The desired physical solution is $\overline{v}_1(x, t) = \text{Real}\{u(x)e^{-i \omega t}\}$, where $u(x) = u'(x) + i u''(x)$ is, in general, complex with real and imaginary parts $u'(x)$ and $u''(x)$, and the time-averaged body force in (17) becomes $\mathcal{F} = \frac{1}{2} \rho_0 \nabla \cdot [u'u' + u''u'']$.

Drawing on the mathematical concepts used in electrophoresis of a spherical particle, explicit solutions for the streaming vorticity and velocity fields can be given in terms of the body force. The derivation is rather tedious but otherwise relatively straightforward and is provided in the Appendix.

IV. EXAMPLES OF THE PRIMARY VELOCITY FIELD

Some representative results will be shown next. In Figs. 1(a)–1(d), we present the real and imaginary parts of the radial and tangential components of the primary velocity from the surface of the sphere at $r/a = 1$ to the far field at $r/a = 15$. Values of the parameters $k_T a$ and $k_L a$ are chosen to reflect the main differences in physical behavior, which are expected to occur if $|k_T a|$ and $|k_L a|$ are larger or smaller compared to unity in different combinations, but subject to the constraint that $|k_L^2| \leq (3/4)|k_T^2|$. The primary flow velocity components are scaled as u_r/U_0 and u_θ/U_0.

Results for the primary velocity field in Figs. 1(a)–1(d) are given for the following four cases:

(i) Both $|k_T a|, |k_L a| \ll 1$, with $k_T a = 0.04 + i0.04$ and $k_L a = 2.5 \times 10^{-3} + i1.35 \times 10^{-5}$ (blue curves). The real parts of u_r and u_θ have large magnitudes and long range, varying monotonically with r/a. The imaginary parts are also monotonic with r/a, but the magnitudes are much smaller than the real parts.

(ii) $|k_T a| \sim 1$ and $|k_L a| \ll 1$, with $k_T a = 0.7 + i0.7$ and $k_L a = 0.05 + i2.7 \times 10^{-4}$ (green curves). The real and imaginary parts of u_r and u_θ have comparable magnitude, but only the real part of u_r is monotonic.

(iii) $|k_T a| \gg 1$ and the real part of $k_L a \sim 1$, but the imaginary part of $k_L a$ is small, with $k_T a = 14 + i14$ and $k_L a = 1.0 + i5.4 \times 10^{-3}$ (red curves). The real and imaginary part of u_r and u_θ all change sign as r/a increases from the sphere surface.

(iv) Both $|k_T a|, |k_L a| \gg 1$, and $k_L a$ has a large imaginary part, with $k_T a = 14 + i14$ and $k_L a = 7.4 + i5.9$ (black curves).
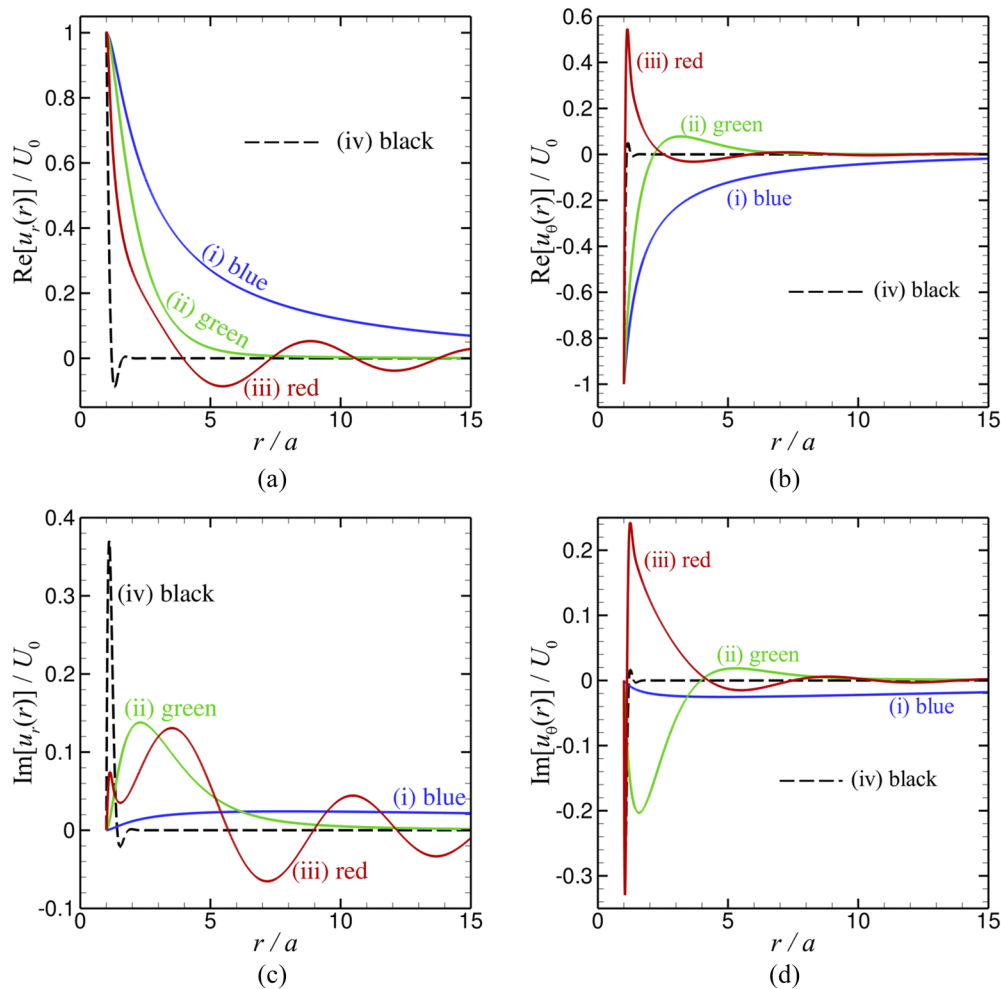
FIG. 1. The primary velocity field for different values of $k_L a$ and $k_T a$, as detailed in the text for cases (i)–(iv): [(a) and (b)] real and [(c) and (d)] imaginary parts of the radial u_r and tangential u_θ primary velocity components, in which $k_T a = 0.04 + i0.04$ and $k_L a = 2.5 \times 10^{-3} + i1.35 \times 10^{-5}$ for case (i), $k_T a = 0.7 + i0.7$ and $k_L a = 0.05 + i2.7 \times 10^{-4}$ for case (ii), $k_T a = 14 + i14$ and $k_L a = 1.0 + i5.4 \times 10^{-3}$ for case (iii), and $k_T a = 14 + i14$ and $k_L a = 7.4 + i5.9$ for case (iv).

In this case, viscous effects dominate, and all flow is confined to within a thin boundary layer adjacent to the sphere surface.

Plots of the primary velocity, $\boldsymbol{u}$, [Eq. (13)] and pressure, p, [Eq. (8)] fields at selected time instants are shown in Fig. 2 (Multimedia view) for case (ii) and in Fig. 3 (Multimedia view) for case (iii). Of special interest are the "vortex-alike" structures appearing to the left and right of Figs. 2(a) and 2(b) (Multimedia view) in the primary flow patterns.

V. RECOVERY OF CLASSICAL SOLUTIONS FOR THE PRIMARY FLOW

In this section, we will investigate several limits for the primary flow field, namely, the small viscosity limit, which will lead to potential flow, the large radius limit leading to the flat plate solution, and the infinite sound speed that together with large viscosity leads to the classical Stokes flow solution.

A. Small viscosity limit, thin boundary layer: Potential flow

If viscous effects are small, we expect a very thin boundary layer. From (6), a vanishing viscosity corresponds to the limit $|k_T a| \gg |k_L a|$, and hence, $e^{ik_T r} \ll 1$ for $r > a$ due to the imaginary part of k_T. From (15), we find
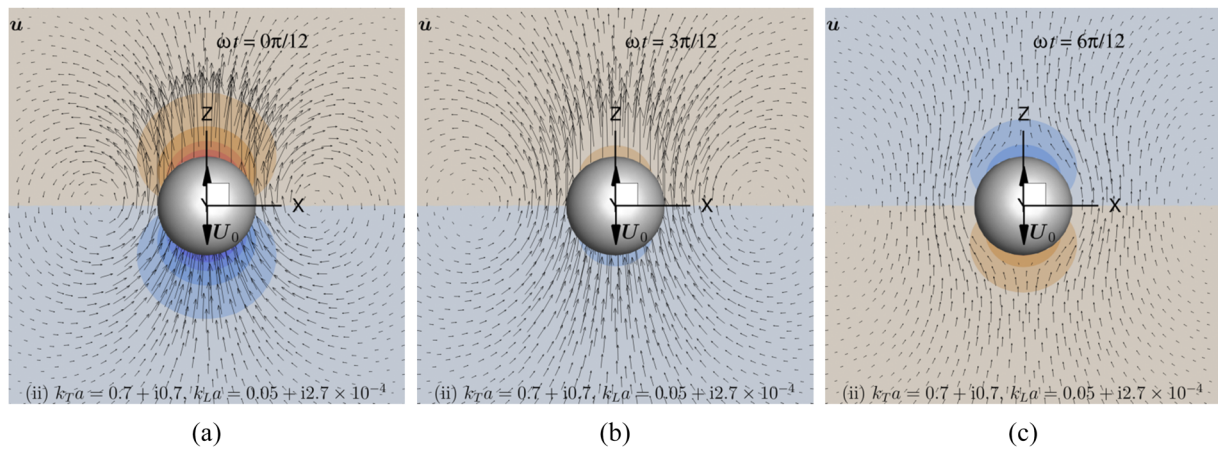
$$\lim_{|k_T a| \to \infty} C_2 = \frac{1}{1 + 2G(k_L a)} e^{-ik_L a}$$

and (13) becomes

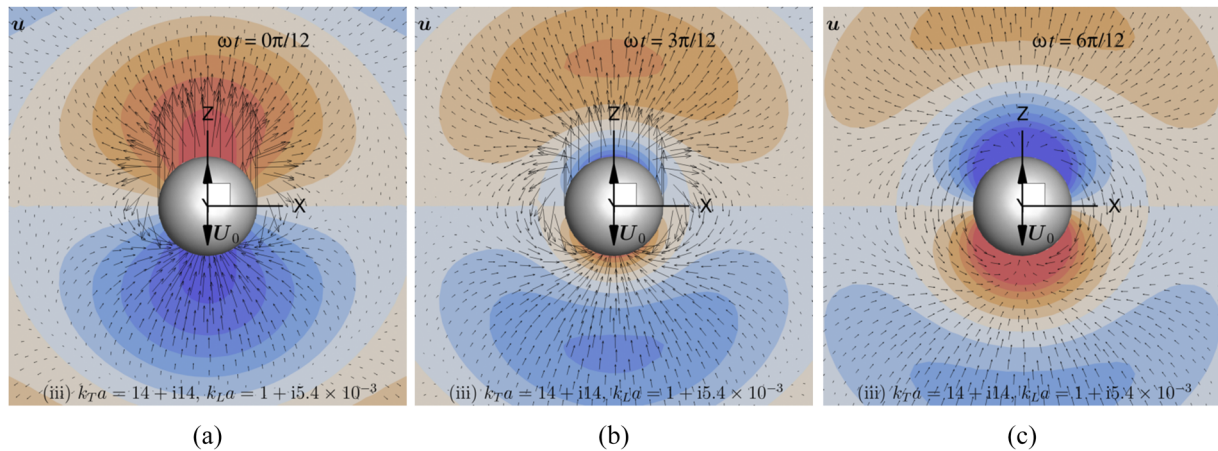$$\lim_{|k_T a| \to \infty} \boldsymbol{u} = \frac{e^{ik_L(r-a)}}{1 + 2G(k_L a)} \frac{a}{r} U_0 \big[\big[1 + 2G(k_L r) \big] \cos\theta \, \boldsymbol{e}_r$$

$$+ \, G(k_L r) \sin\theta \, \boldsymbol{e}_\theta \big]. \qquad (18)$$

This solution is consistent with that given by Landau and Lifshitz[31] (p. 286, Sec. 74, Problem 1).

FIG. 2. Primary flow velocity vector field and pressure distribution (in color) at time frame: (a) $\omega t = 0$, (b) $\omega t = 3\pi/12$, and (c) $\omega t = 6\pi/12$ on the xz plane for case (ii) with $k_T a$ = 0.7 + i0.7 and $k_L a$ = 0.05 + i2.7 × 10^{-4}. Multimedia view: https://doi.org/10.1063/5.0033933.1

FIG. 3. Primary flow velocity vector field and pressure distribution (in color) at time frame: (a) $\omega t = 0$, (b) $\omega t = 3\pi/12$, and (c) $\omega t = 6\pi/12$ on the xz plane for case (iii) when $k_T a$ = 14 + i14 and $k_L a$ = 1.0 + i5.4 × 10^{-3}. Multimedia view: https://doi.org/10.1063/5.0033933.2.

If in addition $|k_L a| \to 0$, we recover the potential flow solution for the fluid velocity around a sphere moving at a constant velocity,

$$\lim_{|k_L a| \to 0\, ;\, |k_T a| \to \infty} \boldsymbol{u} = \frac{a^3}{r^3} U_0 \left[\cos\theta\, \boldsymbol{e}_r + \frac{1}{2} \sin\theta\, \boldsymbol{e}_\theta \right]. \quad (19)$$

This solution is consistent with that given by Landau and Lifshitz[31] (pp. 21–22, Sec. 10, Problem 2).

Figure 4 shows the flow patterns with a carefully selected set of $k_T a$ and $k_L a$ values, $k_T a$ = 14 + i14 and $k_L a$ = 0.05 + i2.7 × 10^{-4}, since it is close to the thin boundary layer limit as $|k_T a| \gg 1$ and $|k_T a| \gg |k_L a|$. As demonstrated in Fig. 4, when $|k_T a| \gg |k_L a|$, outside the thin boundary layer, the results obtained with (13) for the primary velocity field are in good agreement with the results using (18) for the thin boundary layer potential flow limit. In addition, for this particular case, as the imaginary part of $k_L a$ is close to zero, the

imaginary parts of the primary flow velocity components calculated by (18) almost vanish, as displayed by the green circles in Fig. 4. Note that Re[$u_\theta(r)$] closely follows the potential flow results for $r/a > 1.5$ but bends over sharply in the region of $r/a = 1$ to 1.5 to satisfy the no-slip condition of $u_\theta(a) = -1$. In contrast, the potential flow solution is $u_\theta(a) = 0.5$.

B. Large radius: Flat plate limit

If the radius of the sphere, a, is very large, then there are two locations of special interest: the front of the sphere at $\theta = 0$ and the side of the sphere at $\theta = \pi/2$.

Consider first the side at which $\cos\theta = 0$ and $\sin\theta = 1$. From (7), we then find $\boldsymbol{u} = -u_\theta(r)\boldsymbol{e}_z$ since $\boldsymbol{U}_0 = -U_0\boldsymbol{e}_z$. Setting $r/a \to 1$ in (13), we find
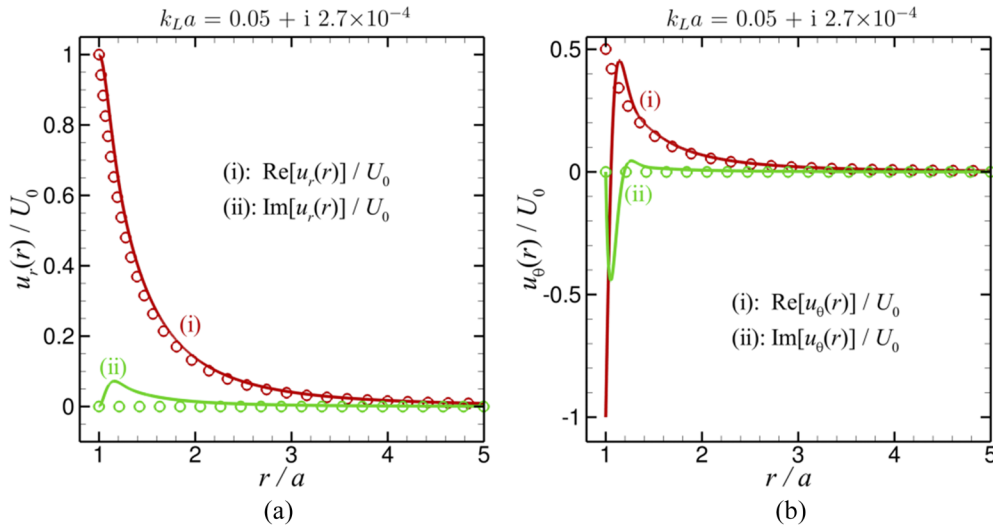
FIG. 4. Comparison of the primary velocity fields at $k_T a = 14 + i14$ and $k_L a = 0.05 + i2.7 \times 10^{-4}$ between the results obtained by using (13) (lines) and those of the thin boundary layer limitation by using (18) (symbols): (a) the radial, u_r, and (b) tangential, u_θ, primary velocity components.

$$\frac{u_\theta(r)}{U_0} = C_1 e^{i k_T r}[1 + G(k_T r)] + C_2 e^{i k_L r} G(k_L r). \qquad (20)$$

For a large sphere, $|k_L a|$, $|k_T a| \gg 1$, so $G(k_L r)$, $G(k_T r) \to 0$ and $C_1 \to -e^{i k_T a}$, and the velocity becomes

$$\lim_{|k_L a|,|k_T a|\to\infty \,;\, \theta=\pi/2} \boldsymbol{u} = -e^{i k_T (r-a)} \boldsymbol{U}_0. \qquad (21)$$

In the time domain, this is equivalent to the well-known Stokes oscillatory boundary thickness equation:[28,32,33] $\boldsymbol{u} = -\boldsymbol{U}_0 e^{-ky} \cos(\omega t - ky)$, with $k = \sqrt{\omega \rho_0/(2\mu)}$, the real part of $k_T = (1 + i)\sqrt{\omega \rho_0/(2\mu)}$, and $y = r - a$ being the distance from the flat surface. Thus, the solution at the side of the sphere tends toward the Stokes vibrating boundary layer theory for a flat plate when the radius of the sphere is large enough.

For the solution in front of the sphere at $\theta = 0$, in the large a or flat plate limit with $\boldsymbol{U}_0 = U_0 \boldsymbol{e}_z$, the velocity in (7) becomes $\boldsymbol{u} = u_r(r) \boldsymbol{e}_z$, and with $a/r \to 1$, we have

$$\frac{u_r(r)}{U_0} = 2 e^{i k_T r} C_1 G(k_T r) + C_2 e^{i k_L r}[1 + 2G(k_L r)]. \qquad (22)$$

Again with $G(k_L r)$, $G(k_T r) \to 0$ for a large sphere, $|k_L a|$, $|k_T a| \gg 1$, we have the limiting solution

$$\lim_{|k_L a|,|k_T a|\to\infty \,;\, \theta=0} \boldsymbol{u} = e^{i k_L (r-a)} \boldsymbol{U}_0, \qquad (23)$$

which represents a plane sound wave propagating out of an oscillating plate.

C. Infinite sound speed: (Oscillatory) incompressible Stokes flow limit

The incompressibility of the fluid implies that $c_0 \to \infty$. In this case, we can take the limit of $|k_L a| \to 0$ while keeping $|k_T a|$ finite.

As such, with the help of the Maclaurin series expansion of $e^{i k_L a}$, we have

$$\lim_{|k_L a|\to 0} C_1 = -\frac{3G(k_L a)}{2G(k_L a)} e^{-i k_T a} \to -\frac{3}{2} e^{-i k_T a}, \qquad (24a)$$

$$\lim_{|k_L a|\to 0} C_2 = \frac{1 + 3G(k_T a)}{e^{i k_L a}[2G(k_L a)]} \to -\frac{(k_L a)^2}{2}[1 + 3G(k_T a)]. \qquad (24b)$$

Introducing (24) into (13), we have

$$\frac{u_\theta(r)}{U_0} = -\frac{3}{2} \frac{a}{r}[1 + G(k_T r)] e^{i k_T (r-a)} + \frac{1 + 3G(k_T a)}{2} \frac{a^3}{r^3}, \qquad (25a)$$

$$\frac{u_r(r)}{U_0} = -3 \frac{a}{r} G(k_T r) e^{i k_T (r-a)} + [1 + 3G(k_T a)]\frac{a^3}{r^3}. \qquad (25b)$$

This solution is identical to the solution given by Landau and Lifshitz[31] (p. 89, Sec. 24, Problem 5), where the velocity was written as $\boldsymbol{u} \equiv \nabla \times \nabla \times [f_L(r) \boldsymbol{U}_0]$; then $u_r(r) = -(2/r)\mathrm{d}f_L(r)/\mathrm{d}r$ and $u_\theta(r) = (1/r)\mathrm{d}f_L(r)/\mathrm{d}r + \mathrm{d}^2 f_L(r)/\mathrm{d}r^2$. They showed that $\frac{\mathrm{d}f_L(r)}{\mathrm{d}r} = a_L\left(\frac{1}{r} - \frac{1}{i k_T r^2}\right) e^{i k_T r} + \frac{b_L}{r^2}$. This corresponds to our solution with $a_L = 3i a e^{-i k_T a}/(2 k_T)$ and $b_L = -[1 + G(k_T a)]a^3/2$. It is also consistent with the solution of Eq. (9) from Ref. 14. As shown in Fig. 5, the results obtained by using (13) for the primary velocity fields at $k_L a = 0.01 + i0.001$ when (i) $k_T a = 1 + i1$ and (ii) $k_T a = 14 + i14$ are in good agreement with the results using (25) for the incompressible Stokes flow limit.

In order to get back the Stokes limit, we have to take the limit $|k_T a| \to 0$ as well. By using the Maclaurin series expansions of $e^{i k_T r}$ and $e^{i k_T a}$, we have
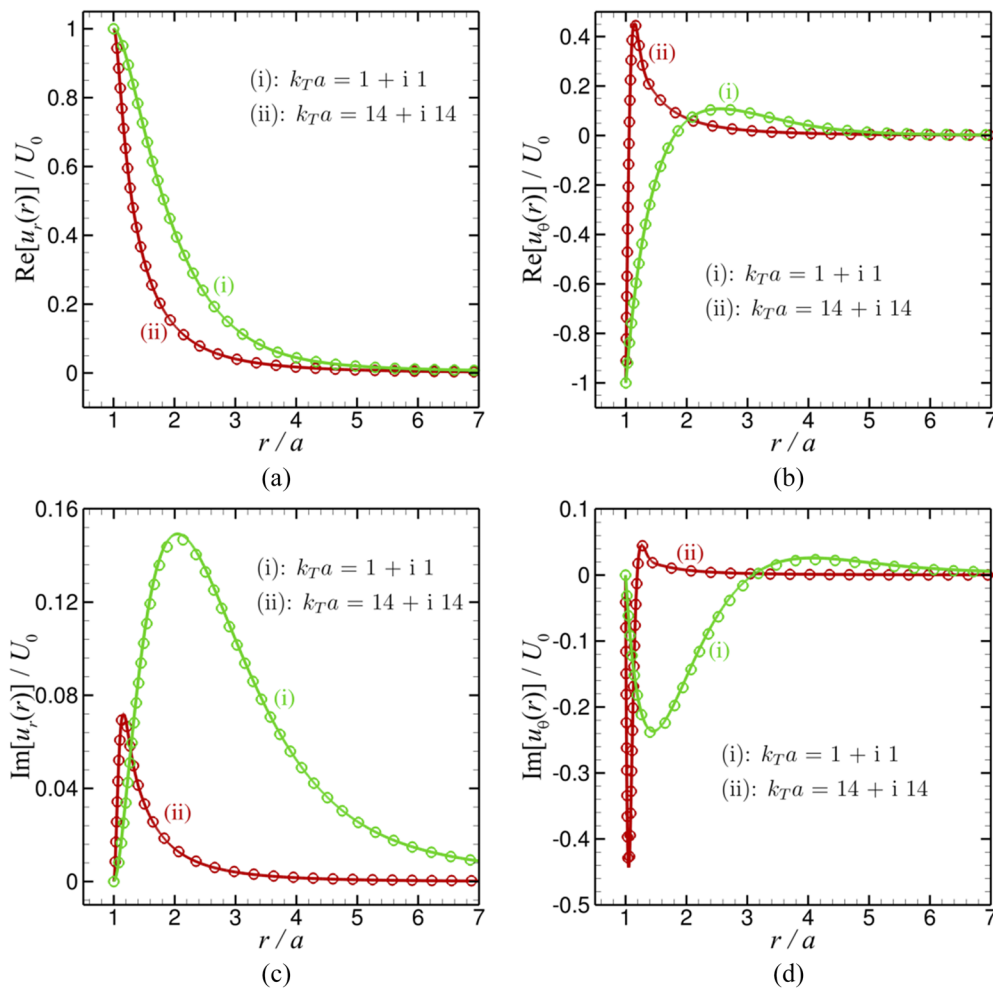
FIG. 5. Comparison of the primary velocity fields at $k_L a = 0.01 + i0.001$ with (i) $k_T a = 1 + i1$ and (ii) $k_T a = 14 + i14$ between the results obtained by using Eq. (13) (lines) and those by using Eq. (25) for the incompressible Stokes flow limit (symbols): [(a) and (b)] real and [(c) and (d)] imaginary parts of the radial, u_r, and tangential, u_θ, primary velocity components.

$$\lim_{|k_T a| \to 0} [1 + G(k_T r)] e^{ik_T r} = \frac{1}{2} - \frac{1}{k_T^2 r^2}, \tag{26a}$$

$$\lim_{|k_T a| \to 0} G(k_T r) e^{ik_T r} = -\frac{1}{2} - \frac{1}{k_T^2 r^2}, \tag{26b}$$

$$\lim_{|k_T a| \to 0} [1 + 3G(k_T a)] e^{ik_T a} = -\frac{1}{2} - \frac{3}{k_T^2 a^2}. \tag{26c}$$

Then, the velocity components become

$$\frac{u_\theta(r)}{U_0} = -\frac{3}{4}\frac{a}{r} + \frac{3}{2k_T^2 r^2}\frac{a}{r} - \frac{1}{4}\frac{a^3}{r^3} - \frac{3}{2k_T^2 a^2}\frac{a^3}{r^3} = -\frac{3}{4}\frac{a}{r} - \frac{1}{4}\frac{a^3}{r^3}, \tag{27a}$$

$$\frac{u_r(r)}{U_0} = \frac{3}{2}\frac{a}{r} + \frac{3}{k_T^2 r^2}\frac{a}{r} - \frac{1}{2}\frac{a^3}{r^3} - \frac{3}{k_T^2 a^2}\frac{a^3}{r^3} = \frac{3}{2}\frac{a}{r} - \frac{1}{2}\frac{a^3}{r^3}, \tag{27b}$$

which is the velocity field for a sphere moving in Stokes flow given by Landau and Lifshitz[31] (pp. 50–60, Sec. 20). Note that in the above-mentioned results, terms with $1/k_T^2$ cancel out each other exactly.

VI. CONCLUSION

The analytical solution of the flow field around a rigid sphere executing small amplitude rectilinear motion in a compressible fluid was investigated. Both the primary flow, where second order inertial effects were neglected, and the secondary flow were studied. The mathematical form of the equation that governs the primary velocity field is identical to that for the propagation of elastic waves in solids. This allows us to draw on earlier work[19] to obtain analytic solutions.

The primary flow field was shown to adhere to all the classical analytical expressions in the small or large viscosity and/or radius limits and is valid for very thin all the way to very thick boundary layers.

The equation that governs the (secondary) streaming flow is analogous to the problem of the flow phenomenon associated with the electrophoretic mobility of a spherical charged particle[23,24] that enables the streaming velocity field to be expressed readily in terms of body force and vorticity.

To the best knowledge of the authors, this is one of the few analytic results in the theory of acoustic boundary layer flow and can serve as a benchmark for numerical solution schemes for more complex problems.

APPENDIX: DERIVATION OF THE SECONDARY FLOW FIELD

In this appendix, the theoretical solution for the secondary flow field is derived, as outlined in Sec. III D.

1. Symmetry of the streaming equation

From the symmetry condition of the primary velocity field in (7), it follows from (17) that the body force per unit volume that drives the streaming flow must be of the form

$$\mathcal{F}(\boldsymbol{x}) = \frac{\rho_0}{4}\left[(\boldsymbol{u}\cdot\nabla)\boldsymbol{u}^* + (\boldsymbol{u}^*\cdot\nabla)\boldsymbol{u} + (\nabla\cdot\boldsymbol{u}^*)\boldsymbol{u} + (\nabla\cdot\boldsymbol{u})\boldsymbol{u}^*\right]$$
$$= \left[F_0(r) + F_2(r)\left(3\cos^2\theta - 1\right)\right]\boldsymbol{e}_r + F_1(r)\cos\theta\,\sin\theta\,\boldsymbol{e}_\theta, \tag{A1}$$

where the superscript "*" denotes the complex conjugate. Explicit expressions for the functions $F_2(r)$, $F_1(r)$, and $F_0(r)$ in (A1) for $\mathcal{F}$ are

$$F_2(r) = \frac{\rho_0}{6}\frac{\mathrm{d}u_r u_r^*}{\mathrm{d}r} + \frac{\rho_0}{12r}\left[2u_\theta u_\theta^* + 3u_\theta u_r^* + 3u_\theta^* u_r + 4u_r u_r^*\right], \tag{A2a}$$

$$F_1(r) = \frac{\rho_0}{4}\frac{\mathrm{d}}{\mathrm{d}r}\left[u_\theta u_r^* + u_\theta^* u_r\right] + \frac{3\rho_0}{4r}\left(2u_\theta u_\theta^* + u_\theta u_r^* + u_\theta^* u_r\right), \tag{A2b}$$

$$F_0(r) = \frac{\rho_0}{6}\frac{\mathrm{d}u_r u_r^*}{\mathrm{d}r} + \frac{\rho_0}{12r}\left[4u_r u_r^* - 4u_\theta u_\theta^*\right]. \tag{A2c}$$

Using this general form for $\mathcal{F}(\boldsymbol{x})$ in (17), the streaming velocity must have the following angular and radial dependency:

$$\boldsymbol{U}(\boldsymbol{x}) = U_r(r)\left(3\cos^2\theta - 1\right)\boldsymbol{e}_r + U_\theta(r)\cos\theta\,\sin\theta\,\boldsymbol{e}_\theta$$
$$= \frac{S(r)}{r}\left(3\cos^2\theta - 1\right)\boldsymbol{e}_r - \frac{1}{r}\frac{\mathrm{d}}{\mathrm{d}r}\left[rS(r)\right]\cos\theta\,\sin\theta\,\boldsymbol{e}_\theta. \tag{A3}$$

The condition $\nabla\cdot\boldsymbol{U}(\boldsymbol{x}) = 0$ (see the works of Nyborg[21] and Lee and Wang[18]) ensures that the streaming velocity is determined by the single function $S(r)$ in (A3). The form for the pressure can be inferred from (17),

$$P(\boldsymbol{x}) = P_0(r) + P_2(r)(3\cos^2\theta - 1). \tag{A4}$$

Instead of solving for the three functions $S(r)$, $P_0(r)$, and $P_2(r)$, it is more convenient to work in terms of the vorticity field, $\boldsymbol{W} = \nabla \times \boldsymbol{U}$, to eliminate the pressure, $P(\boldsymbol{x})$. We hereby follow very closely the theory used for electrophoresis of a moving sphere, in particular that of the Ph.D. thesis of Overbeek;[23] although the theory is not identical, many of the mathematical concepts such as vector manipulation in spherical coordinates and double integration techniques can still be utilized here. Taking the curl of (17) gives $\nabla \times \mathcal{F} = \mu\nabla^2\boldsymbol{W}$. Since both the body force $\mathcal{F}$ and the streaming velocity $\boldsymbol{U}$ are independent of the azimuthal angle φ and have no azimuthal φ-component, their curl will only have a non-zero component in the φ-direction along the unit vector, $\boldsymbol{e}_\varphi$. This then ensures that $\nabla^2\boldsymbol{W}$ also points in the φ direction. From (A1) and (A3), they are characterized by two functions, $f(r)$ and $W(r)$, that are only functions of the radial distance r from the center of the sphere,

$$\nabla \times \mathcal{F}(\boldsymbol{x}) = f(r)\cos\theta\,\sin\theta\,\boldsymbol{e}_\varphi, \tag{A5}$$

$$\boldsymbol{W}(\boldsymbol{x}) \equiv \nabla \times \boldsymbol{U}(\boldsymbol{x}) = W(r)\cos\theta\,\sin\theta\,\boldsymbol{e}_\varphi, \tag{A6}$$

with $f(r)$ that characterizes the body force in (A5) given by

$$f(r) = \frac{1}{r}\left\{\frac{\mathrm{d}}{\mathrm{d}r}\left[rF_1(r)\right] + 6F_2(r)\right\}. \tag{A7}$$

This completes the framework of the axisymmetric streaming flow around a sphere.

2. Formal solution of the streaming equation

The method of solution involves deriving an ordinary differential equation for $W(r)$ defined in (A6) in terms of $f(r)$ defined in (A5). Then, the velocity function $S(r)$ given by (A3) can be expressed in terms of $W(r)$ to give the solution for the velocity field.

Expressing $\nabla^2\boldsymbol{W}(\boldsymbol{x})$ in spherical polar coordinates, the curl of (17) becomes

$$f(r) = \mu r\frac{\mathrm{d}}{\mathrm{d}r}\left[\frac{1}{r^4}\frac{\mathrm{d}}{\mathrm{d}r}\left(r^3 W(r)\right)\right] \tag{A8}$$

that can be integrated immediately to give the vorticity function, $W(r)$; noting that $W(r) \to 0$ as $r \to \infty$,

$$W(r) = \frac{c_w}{r^3} + W_f(r),$$

with

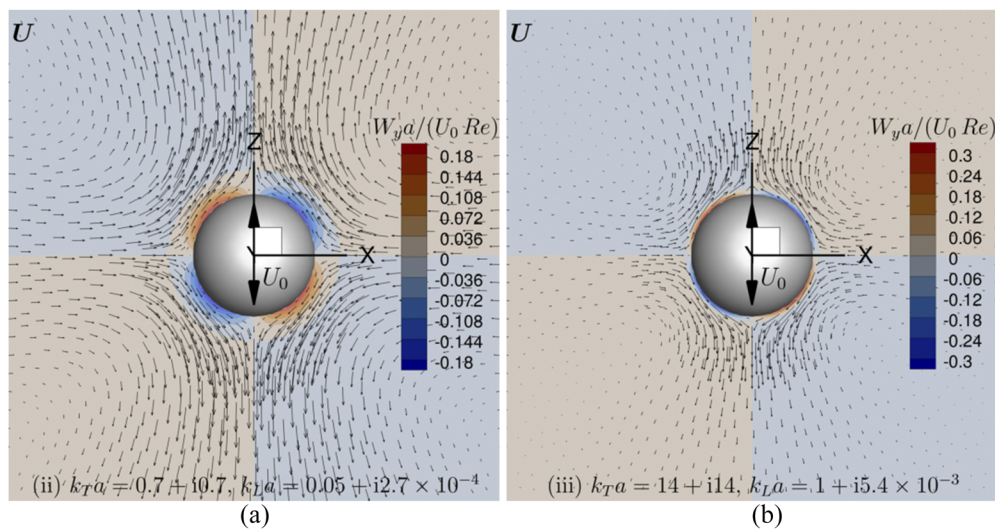$$W_f(r) \equiv \frac{1}{\mu}\frac{1}{r^3}\int_r^\infty y^4\left[\int_y^\infty \frac{f(x)}{x}\mathrm{d}x\right]\mathrm{d}y. \tag{A9}$$

The integration constant c_w from the homogeneous solution can be determined from the boundary conditions at the sphere surface $r = a$.

In a similar way, the streaming velocity function $S(r)$ can be found by combining (A3) and (A6) to give

$$W(r) = -r\frac{\mathrm{d}}{\mathrm{d}r}\left[\frac{1}{r^4}\frac{\mathrm{d}}{\mathrm{d}r}\left[r^3 S(r)\right]\right] \tag{A10}$$

FIG. 7. The secondary flow velocity vector and vorticity distribution on the xz plane for (a) case (ii) with $k_T a = 0.7 + i0.7$ and $k_L a = 0.05 + i2.7 \times 10^{-4}$ and (b) case (iii) when $k_T a = 14 + i14$ and $k_L a = 1.0 + i5.4 \times 10^{-3}$.

defined as $Re = \rho_0 a U_0 / \mu$. Thus, the time-averaged body force $f(r)$ is significant only within a thin boundary layer from the sphere surface, and this is reflected in the observation that the vorticity $W(r)$ is non-zero only within about 5 radii from the surface. However, the streaming velocity field can extend well beyond the range of the streaming vorticity with the typical long ranged characteristics of Stokes flow around a sphere.

Plots of the secondary velocity, U, and vorticity, W_y, are shown in Fig. 7 for cases (ii) and (iii). The four-lobed velocity profile is clearly visible in Fig. 7 for the secondary streaming flow. Also clearly visible are the eight regions of the secondary streaming flow vorticity W_y in Fig. 7. Even though the vorticity changes sign in each quadrant, the secondary streaming flow velocity does not reverse direction in an individual quadrant. Near the sphere, the axially symmetric steady acoustic streaming flow U due to oscillatory motion of the sphere in the z direction draws fluid toward the sphere in the xy-plane and re-directs the fluid away from the sphere symmetrically along the $\pm z$ directions.

DATA AVAILABILITY

The data that support the findings of this study are available from the corresponding author upon reasonable request.

REFERENCES

[1] T. Laurell and A. Lenshof, *Microscale Acoustofluidics* (The Royal Society of Chemistry, Cambridge, UK, 2015).

[2] P. Muller and H. Bruus, "Theoretical study of time-dependent, ultrasound-induced acoustic streaming in microchannels," Phys. Rev. E **92**, 063018 (2015).

[3] J. Lei, P. Glynne-Jones, and M. Hill, "Modal Rayleigh-like streaming in layered acoustofluidic devices," Phys. Fluids **28**, 012004 (2016).

[4] A. A. Doinikov, P. Thibault, and P. Marmottant, "Acoustic streaming induced by two orthogonal ultrasound standing waves in a microfluidic channel," Ultrasonics **87**, 7–19 (2018).

[5] J. T. Karlsen, W. Qiu, P. Augustsson, and H. Bruus, "Acoustic streaming and its suppression in inhomogeneous fluids," Phys. Rev. Lett. **120**, 054501 (2018).

[6] J. S. Bach and H. Bruus, "Suppression of acoustic streaming in shape-optimized channels," Phys. Rev. Lett. **124**, 214501 (2020).

[7] S. Subbotin, V. Kozlov, and M. Shiryaeva, "Effect of dimensionless frequency on steady flows excited by fluid oscillation in wavy channel," Phys. Fluids **31**, 103604 (2019).

[8] K. Pandey, D. Prabhakaran, and S. Basu, "Review of transport processes and particle self-assembly in acoustically levitated nanofluid droplets," Phys. Fluids **31**, 112102 (2019).

[9] T. Baasch, A. A. Doinikov, and J. Dual, "Acoustic streaming outside and inside a fluid particle undergoing monopole and dipole oscillations," Phys. Rev. E **101**, 013108 (2020).

[10] F. Otto, E. K. Riegler, and G. A. Voth, "Measurements of the steady streaming flow around oscillating spheres using three dimensional particle tracking velocimetry," Phys. Fluids **20**, 093304 (2008).

[11] J. Karlsen and H. Bruus, "Forces acting on a small particle in an acoustical field in a thermoviscous fluid," Phys. Rev. E **92**, 043010 (2015).

[12] J. S. Marshall and J. Wu, "Acoustic streaming, fluid mixing, and particle transport by a Gaussian ultrasound beam in a cylindrical container," Phys. Fluids **27**, 103601 (2015).

[13] C. A. Lane, "Acoustical streaming in the vicinity of a sphere," J. Acoust. Soc. Am. **27**, 1082–1086 (1955).

[14] N. Riley, "On a sphere oscillating in a viscous fluid," Q. J. Mech. Appl. Math. **19**, 461–472 (1966).

[15] B. J. Davidson and N. Riley, "Cavitation microstreaming," J. Sound Vib. **15**, 217–233 (1971).

[16] M. S. Longuet-Higgins, "Viscous streaming from an oscillating spherical bubble," Proc. R. Soc. London, Ser. A **454**, 725–742 (1998).

[17] N. Riley, "Steady streaming," Annu. Rev. Fluid Mech. **33**, 43–65 (2001).

[18] C. P. Lee and T. G. Wang, "Outer acoustic streaming," J. Acoust. Soc. Am. **88**, 2367–2375 (1990).

[19] E. Klaseboer, Q. Sun, and D. Y. C. Chan, "Helmholtz decomposition and boundary element method applied to dynamic linear elastic problems," J. Elasticity **137**, 83–100 (2019).

[20] J. T. Stuart, "Double boundary layers in oscillatory viscous flow," J. Fluid Mech. **24**, 673–687 (1966).

[21] W. L. Nyborg, "Acoustic streaming due to attenuated plane waves," J. Acoust. Soc. Am. **25**, 68–75 (1953).

[22] Lord Rayleigh, *The Theory of Sound* (Dover Publications, New York, 1877), Vol. 1.

[23] J. T. G. Overbeek, "Theorie der electrophorese," Ph.D. thesis, Utrecht University, H.J. Paris, Amsterdam (1941); arXiv:1907.05542.

[24] A. S. Jayaraman, E. Klaseboer, and D. Y. C. Chan, "The unusual fluid dynamics of particle electrophoresis," J. Colloid Interface Sci. **553**, 845–863 (2019).

[25] C. Eckart, "Vortices and streams caused by sound waves," Phys. Rev. **73**, 68–76 (1948).

[26] A. Gopinath and E. H. Trinh, "Compressibility effects on steady streaming from a noncompact rigid sphere," J. Acoust. Soc. Am. **108**, 1514–1520 (2000).

[27] P. Hahn, J. Wang, and J. Dual, "A parallel boundary element algorithm for the computation of the acoustic radiation forces on particles in viscous fluids," in Proceedings of the 2013 International Conference on Ultrasonics (ICU 2013), Singapore, May 2-5, 2013.

[28] H. Schlichting, *Boundary-Layer Theory* (McGraw-Hill, 1955).

[29] S. S. Sadhal, *Microscale Acoustofluidics* (The Royal Society of Chemistry, 2015), Chap. 12, pp. 256–311.

[30] L. D. Landau and E. M. Lifshitz, *Theory of Elasticity*, 2nd ed. (Pergamon Press, Great Britain, 1970).

[31] L. D. Landau and E. M. Lifshitz, *Fluid Mechanics*, 2nd ed. (Pergamon Press, Great Britain, 1987).

[32] G. G. Stokes, "On the effect of the internal friction of fluids on the motion of pendulums," Trans. Camb. Phil. Trans. **9**, 8 (1851).

[33] E. Ramos, S. Cuevas, and G. Huelsz, "Interaction of Stokes boundary layer flow with a sound wave," Phys. Fluids **13**, 3709–3713 (2001).